

RESEARCH ARTICLE

# Anthocyanin rich extract of *Brassica oleracea* L. alleviates experimentally induced myocardial infarction

Sarmita Jana<sup>1</sup>✉, Dipak Patel<sup>1,2</sup>✉, Shweta Patel<sup>1</sup>, Kapil Upadhyay<sup>1</sup>, Jaymesh Thadani<sup>1</sup>, Rahul Mandal<sup>3</sup>, Santasabuj Das<sup>3</sup>, Ranjitsinh Devkar<sup>1</sup>\*

**1** Phytotherapeutics and Metabolic Endocrinology Division, Department of Zoology, Faculty of Science, The M.S. University of Baroda, Vadodara, India, **2** Ecotoxicology lab, Jai Research Foundation, Vapi, India, **3** Biomedical Informatics centre, National Institute of Cholera and Enteric Diseases, Kolkata, India

✉ These authors contributed equally to this work.

\* [rv.devkar-zoo@msubaroda.ac.in](mailto:rv.devkar-zoo@msubaroda.ac.in)



**OPEN ACCESS**

**Citation:** Jana S, Patel D, Patel S, Upadhyay K, Thadani J, Mandal R, et al. (2017) Anthocyanin rich extract of *Brassica oleracea* L. alleviates experimentally induced myocardial infarction. PLoS ONE 12(8): e0182137. <https://doi.org/10.1371/journal.pone.0182137>

**Editor:** Suresh Yenugu, University of Hyderabad, INDIA

**Received:** March 12, 2017

**Accepted:** July 12, 2017

**Published:** August 1, 2017

**Copyright:** © 2017 Jana et al. This is an open access article distributed under the terms of the [Creative Commons Attribution License](https://creativecommons.org/licenses/by/4.0/), which permits unrestricted use, distribution, and reproduction in any medium, provided the original author and source are credited.

**Data Availability Statement:** All relevant data are within the paper and its Supporting Information files.

**Funding:** This study was supported by the University Grant Commission, providing financial assistance in form of Major Research Project (F. No.41-89/2012/SR).

**Competing interests:** The authors have declared that no competing interests exist.

## Abstract

Cardioprotective potential of anthocyanin rich red cabbage extract (ARCE) was assessed in H<sub>2</sub>O<sub>2</sub> treated rat neonatal cardiomyoblasts (H9c2 cells) and isoproterenol (ISO) induced rodent model of myocardial infarction. H<sub>2</sub>O<sub>2</sub> treated H9c2 cells recorded cytotoxicity (48–50%) and apoptosis (57.3%), the same were reduced in presence of ARCE (7–10% & 12.3% respectively). Rats pretreated with ARCE for 30 days followed by ISO treatment recorded favourable heart: body weight ratio as compared to ISO treated group. Also, the mRNA levels of enzymatic antioxidants (*sod* and *catalase*) and apoptotic genes (*bax* and *bcl-2*) in ARCE+ISO treated group were similar to the control group suggesting that ARCE pretreatment prevents ISO induced depletion of enzymatic antioxidants and apoptosis. Histoarchitecture of ventricular tissue of ISO treated group was marked by infarcted areas (10%) and derangement of myocardium whereas, ARCE+ISO treated group (4.5%) recorded results comparable to control (0%). ARCE+ISO treated group accounted for upregulation of *caveolin-3* and *SERCA2a* expression as compared to the ISO treated group implying towards ARCE mediated reduction in membrane damage and calcium imbalance. Molecular docking scores and LigPlot analysis of cyanidin-3-glucoside (-8.7 Kcal/mol) and delphinidin-3-glucoside (-8.5 Kcal/mol) showed stable hydrophobic and electrostatic interactions with β<sub>1</sub> adrenergic receptor. Overall this study elucidates the mechanism of ARCE mediated prevention of experimentally induced myocardial damage.

## Introduction

Cardiovascular diseases (CVDs) cause significant morbidity and continue to remain the leading cause of death globally. Myocardial infarction (MI) is the most prevalent type of CVD wherein loss of cardiomyocytes due to apoptosis is at the epicentre of its pathogenesis [1]. Reactive oxygen species (ROS) mediated depletion of intracellular antioxidants, lipid peroxidation, modification of structural proteins and DNA damage precede apoptosis. Therefore,

reduction of intracellular ROS is one of the key targets of research to regulate apoptotic cascade in cardiomyocytes [2]. Rat cardiomyocytes when treated with H<sub>2</sub>O<sub>2</sub>, undergo cellular damage due to production of free radicals wherein, the sequences of events are similar to an oxidatively stressed myocardium. Isoproterenol (ISO) is a synthetic  $\beta$  adrenergic agonist that causes myocardial hyperactivity, coronary hypotension hypoxia [3], calcium overload and infarct like necrosis [4]. Therefore, H<sub>2</sub>O<sub>2</sub> induced oxidative stress and ISO induced myocardial infarction models are used to assess cardioprotective potential of the test compounds [5, 6]

Anthocyanins (a member of flavonoid family) are polyhydroxyl and polymethyl derivatives of flavinium salts that have been extensively reported to manifest therapeutic properties against alzheimer's disease [7], hyperlipidaemia [8], hyperglycaemia [9], cardiovascular diseases [10], diabetic retinopathy [11] and in lowering blood pressure [12]. Red cabbage (*Brassica oleracea* L; Family-Brassicaceae) is a commonly consumed functional food in Asia and Europe due to its low calorie-high fibre composition [13]. It is also a rich source of anthocyanins such as cyanidin-3-diglucoside-5-glucoside and their various acylated derivatives [14, 15]. Reports on its hepatoprotective [16], membrane stabilizing [17] and neuroprotective [18] potentials have been published wherein, therapeutic potential of red cabbage has been attributed to high content of anthocyanins. Previous studies in our lab had reported that co-supplementation of Anthocyanin rich Red Cabbage Extract (ARCE) prevents cardiac and hepatic oxidative stress in atherogenic diet fed rats [19] and improves mitochondrial membrane potential in oxidatively stressed cardiomyoblasts [20]. Though, consumption of anthocyanin in reducing cardiovascular risks and myocardial infarction [21] has been reported, ARCE has not been investigated in detail for its cardioprotection.

Extensive reports on cardioprotective potential of anthocyanins and leads from our previous study on ARCE prompted us to initiate a detailed investigation. Study showcased herein, assesses the mechanism of cardioprotective potential by ARCE via *in vitro*, *in vivo* and *in silico* models.

## Materials and methods

### Materials

All chemicals of molecular biology grade were purchased commercially. Methanol, dimethyl sulfoxide (DMSO), 3-(4,5-dimethylthiazol-2-yl)-2,5-diphenyl tetrazolium bromide (MTT) were purchased from Sisco Research Laboratory Pvt. Ltd. (Mumbai, India). Triphenyl tetrazolium chloride (TTC) stain, hematoxylin, eosin and isoproterenol (ISO) were purchased from Sigma-Aldrich (St. Louis, MO, USA). Fetal bovine serum (FBS), Dulbecco's Modified Eagle's Medium (DMEM), trypsin phosphate versene glucose (TPVG) and antibiotic-antimycotic solution were purchased from Hi-media Laboratories (Mumbai, India). Annexin V-Alexa 488, Propidium Iodide (PI), TRIzol reagent, DreamTaq Green master mix and SYBR select master mix were procured from Invitrogen (CA, USA). iScript cDNA synthesis kit was purchased from Bio-Rad (CA, USA). ENZOPAK Creatine Kinase-Myocardial b fraction (CK-MB) kit was purchased from Reckon Diagnostics (Vadodara, Gujarat). RNAlater stabilizing solution was purchased from Ambion Inc. (USA).

### Preparation of ARCE

Red cabbage (*Brassica oleracea* L. var. Capitata f. rubra DC.) was procured from Spencer's mall, Vadodara, Gujarat, India (22° 19' 21" N, 73° 10' 32" E), identified and authenticated by Dr. Vinay Raole, Department of Botany and voucher specimen (accession no. 213) was submitted to departmental herbarium (BARO), The M. S. University of Baroda, Vadodara, Gujarat. Fresh red cabbage was chopped into small pieces and extracted using methanol: water:

HCl (50:50:1) solvent system. The resultant extract was dried in rotatory evaporator at 40°C, cooled at room temperature and stored at 4°C till further analysis [22]. The resultant yield (7.1% w/w) was diluted with distilled water and the total Anthocyanin content was measured spectrophotometrically using molar extinction coefficient of cyanidin-3,5-diglucoside (26,300 M<sup>-1</sup> cm<sup>-1</sup>).

## Identification of anthocyanins in ARCE

Anthocyanins were identified by Thin Layer Chromatography (TLC) and gas Chromatography/ Mass spectroscopy (GC/MS). Briefly, methanolic solution of ARCE (40mg/ml) was subjected to TLC (Silica gel 60 F<sub>254</sub>) and developed in a pre-saturated chamber of Ethyl acetate: Glacial acetic acid: Formic acid: H<sub>2</sub>O (10: 1.1: 1.1: 2.6). Plates were dried at room temperature and bands were scraped using a clean scalpel. The contents were dissolved in 5 ml methanol and filtered (Whatman Filter paper No. 1). Filtrates were dried in rotatory evaporator (40°C), cooled to room temperature and stored at 4°C till further analysis. Sample (2.5 mg/ml methanol) was injected through pre-filter unit using Helium gas (99.9% gas carrier) with a flow rate of 1ml/min. The column (30m PE-5ms) temperature was held at 60°C for 5min and then increased up to 280°C at the rate of 10°C/min. Mass spectra were scanned from 10 to 610 u.

## Experimental design

**Maintenance of H9c2 cells.** Rat cardiomyoblasts (H9c2 cells) were procured from National Centre for Cell Science (NCCS, Pune, India) and maintained at 37°C with 5% CO<sub>2</sub> in DMEM (10% FBS and 1% antibiotic antimycotic solution). Cells were trypsinized using 1X TPVG at every third day. The study was grouped as Control (untreated cells), ARCE (treated with 250 µg/ml ARCE for 24 h), H<sub>2</sub>O<sub>2</sub> (100 µM for 12 h) and ARCE+ H<sub>2</sub>O<sub>2</sub> (pre-treated with ARCE for 24 h followed by H<sub>2</sub>O<sub>2</sub> for 12 h).

**Cytotoxicity assay.** H9c2 cells were seeded in 96 well plate (10<sup>4</sup> cells/well), allowed to grow overnight and were treated as mentioned above. MTT (5 mg/ml) was added in each well and incubated in dark for 4 h. The resultant purple formazan crystals were dissolved in DMSO (150 µl/well) and absorbance was measured at 540nm using ELX800 universal Microplate Readers (Bio-Tek instruments, Inc., Winooski, VT) and % cytotoxicity was calculated with respect to control.

**Apoptosis assay.** Cells (1×10<sup>4</sup>) of various groups were trypsinized, centrifuged and washed with PBS. Control and treated cells were stained with AnnexinV-Alexa 488 and Propidium Iodide for 15 min at 37°C in dark [23] and subjected to flow cytometric analysis. The data were acquired using BD FACSAria™ III (BD Biosciences, USA).

**Experimental animals.** Adult albino male Charles foster rats (n = 36, 160–180 g) were obtained from Department of Biochemistry, The M.S. University of Baroda, Vadodara, India. Throughout the study, rats were maintained in clean polypropylene cages and controlled conditions (23±2°C, LD 12:12 and 45–50% humidity with food and water *ad libitum*) as per standard guidelines of Committee for the Purpose of Control and Supervision of Experiments on Animals (CPCSEA). The experimental protocol (P.N.3approval no. 827/ac/04/CPCSEA) was approved by the Institutional Animal Ethics Committee (IAEC) and the Committee for the Purpose of Control and Supervision of Experiments on Animals (reg. no. 827/ac/04/CPCSEA) of the Department of Zoology, The M. S. University of Baroda, Vadodara, Gujarat, India. Rats were acclimatized for 10 days prior to setting up of the experiment. During the entire period of study, the health condition of rats was closely monitored for any possible injury and abnormal behaviour. Weekly records of food consumption and body weight were maintained.

**Isoproterenol (ISO) model of myocardial infarction.** Rats were randomly divided into three groups of six animals each and dosed via gastric intubation as follows. Group 1 (Control): normal saline daily for 30 days. Group 2 (Disease control): normal saline daily for 28 days followed by Isoproterenol (ISO: 85 mg/kg body weight *s.c.*) on 29<sup>th</sup> and 30<sup>th</sup> day. Group 3 (ARCE+ISO): ARCE (250 mg/kg body weight) daily for 28 days and Isoproterenol (ISO: 85 mg/kg body weight *s.c.*) on 29<sup>th</sup> and 30<sup>th</sup> day. At the end of the experimental period (31<sup>st</sup> day) rats were fasted overnight (12h). The next day, rats were anaesthetised with 1% pentobarbital sodium (40 mg/kg, *i.p.*) and blood samples were collected from retro-orbital sinus puncture. Blood samples were centrifuged at 3000 rpm for 10 min at 4°C and plasma was stored at -20°C till further analysis. Animals were sacrificed by decapitation and whole hearts (6 per group) were excised and weighed. Ratio of heart: body weight (cardiosomatic index) was calculated [24]. Some part of the ventricular tissue (~50 mg) was cut from each heart and fixed in RNAlater stabilization solution at -20°C. The remaining ventricular tissue was horizontally divided into two parts for histopathology and study of infarcted area respectively.

**Gene expression studies.** Cardiac tissue samples collected in RNAlater stabilization solution were washed with DEPC water. Total RNA was isolated using TRIzol reagent. cDNA was synthesized by reverse transcription of total RNA (1 µg) using iScript cDNA Synthesis kit. Further, mRNA levels of enzymatic antioxidants (superoxide dismutase; *sod* and *catalase*), apoptotic genes (*bax* and *bcl-2*), myocardium specific caveolae protein (*caveolin-3*), and sarco/endoplasmic reticulum calcium ATPases (*SERCA2a*) with *GAPDH* as an internal control were evaluated by quantitative PCR as elucidated herein.

Quantitative PCR analysis (QuantStudio 12K Flex, Life Technologies, CA, USA) was performed using SYBR Select Master Mix. The reaction mixture consisted of cDNA (0.8 µl), forward and reverse primers (0.4 µl each), SYBR green master mix (5 µl) and ultrapure water (3.4 µl). Melting curve of each sample was measured to ensure the specificity of the products. The data were normalized to the internal control *GAPDH* and analysed using  $2^{-\Delta\Delta CT}$  method [25]. Primers used for this study are listed in Table 1.

**Plasma CK-MB.** Plasma samples were thawed and activity levels of CK-MB enzyme were estimated in control and treated samples as per the instruction manual of ENZOPAK CK-MB kit.

**Microscopic and macroscopic evaluation of cardiac tissue.** Tissue samples of ventricle (control and treated) were fixed in 10% buffered paraformaldehyde after autopsy. Later, tissue samples were dehydrated with series of graded alcohol and embedded in paraffin wax. Tissue sections (5 µm) were cut, mounted onto slides and stained with haematoxylin and eosin (H&E) and photographed (Leica DM 2000) at 100X and 400X. Fresh transverse ventricular slices (1–2 mm) were stained with 2,3,5-triphenyltetrazolium chloride (TTC) at 37°C for 20 min and photographed using Canon power S70 shot digital camera [26]. The % infarct area of

**Table 1. Primers for quantitative PCR.**

Gene Name	Accession number	Forward Primer (5'→3')	Reverse Primer (5'→3')	Product length
<i>GAPDH</i>	NM_017008.4	actttggcatcgtggaagg	acttggcaggtttctccagg	264 bp
<i>sod</i>	NM_017051.2	gacattgtgcctctgggttt	gccctgcatactttgtccat	114 bp
<i>catalase</i>	NM_012520.2	gaggaaacgcctgtgtgaga	ttggcagctatgtgagagcc	201 bp
<i>bax</i>	NM_0170592	gctggacactggacttcctc	ctcagcccatcttctccag	168 bp
<i>bcl-2</i>	NM_016993.1	tctcatgccaaaggggaaac	tatcccactcgtagcccctc	192 bp
<i>caveolin-3</i>	NM_019155.2	ggcaccgatcatcaaggaca	acacgccatcgaagctgtaa	177 bp
<i>SERCA2a</i>	NM_001110139.2	caacacatcttccagccctct	acttggctgatggcttctgtt	246 bp

<https://doi.org/10.1371/journal.pone.0182137.t001>

the ventricles was measured using Image J software (NIH, USA). Whereas, the ventricular thickness was measured using an occlusometer [27].

**Homology modelling and molecular docking.** The sequence of Rat  $\beta_1$  adrenergic receptor ( $\beta_1$ AR) was retrieved from NCBI sequence database (accession number NP\_036833 XP\_001063787) and the 3D model was generated using CPHmodels-3.2 Server. Further the stereochemical quality of the modelled structure was evaluated through Ramachandran plot. Molecular docking of delphinidin-3-glucoside and cyanidin-3-glucoside with Rat  $\beta_1$ AR model was performed using Glide program in Schrodinger and calculations were done using Extra Precision (XP) method. The protein and the ligand molecules were prepared for docking using Protein Preparation Wizard and LigPrep respectively, available in Schrodinger suite. A 20 Å grid box was generated at the active site of the  $\beta_1$ AR using three active site residues N352, S228 and D138. Information of these three residues was retrieved from the co-crystal structure of quinoline with Turkey  $\beta_1$ AR (PDB ID: 3ZPR). PyMol was used for visualization of molecular interactions.

**Statistical analysis.** The data were expressed as mean  $\pm$  SEM and analyzed by one way analysis of variance (ANOVA) using Graph Pad Prism 3.0 (CA, USA).  $P < 0.05$  were considered to be significant.

## Results

### Anthocyanin content

Total anthocyanin content in ARCE was found to be  $86.004 \pm 3.103$  mg/100gm. TLC of ARCE revealed two bands with  $R_f$  value 0.26 and 0.31 respectively. These values were in the  $R_f$  value range of 0.2–0.35 and which indicate presence of monoglucosides delphinidin-3-glucoside and cyanidin-3-glucoside [28] (Fig 1A). The GC-MS spectra provided information regarding the structural identification of anthocyanin pigments. The  $m/z$  ratio of the daughter and parents ions, confirmed the presence of anthocyanins. Analysis of crude extract (S1A Fig and Fig 1B, Table 2) showed presence of cyanidin-3-glucoside (449  $m/z$ ) and Delphinidin-3-glucoside (465  $m/z$ ). Whereas, analysis of bands obtained from TLC showed presence of daughter ions of (epi) gallocatechin delphinidin (303 and 481  $m/z$ ), (epi) gallocatechin peonidin glucoside (605  $m/z$ ), peonidin glucoside (463  $m/z$ ) in the first band (S1B Fig and Fig 1C, Table 3) and Cyanidin (287  $m/z$ ), Cyanidin-3(6"-acetyl glucoside) (491  $m/z$ ), Cyanidindioxaly Glucoside (593  $m/z$ ), Delphinidin-3(6"-acetyl glucoside) (507  $m/z$ ) and delphinidin-3-glucoside (465  $m/z$ ) in second band (S1C Fig and Fig 1D, Table 4). Overall, presence of cyanidin and delphinidin monoglucosides were recorded in ARCE.

### Cytotoxicity and flowcytometry analysis

ARCE was non toxic but  $H_2O_2$  treatment accounted for 48–50% cytotoxicity in H9c2 cells. However, ARCE+ $H_2O_2$  group accounted for a decrement in cytotoxicity in a dose dependent manner (Fig 2). Also, ARCE treatment accounted for less number of apoptotic cells (12.3%) as compared to  $H_2O_2$  treated cells (57.3%). However, ARCE+ $H_2O_2$  group accounted for a decrement in apoptosis (19.1%) comparable to that of control or ARCE treated cells (Fig 3)

### Gene expression studies in H9c2 cells

mRNA levels of enzymatic antioxidants (*sod* and *catalase*) were downregulated in  $H_2O_2$  treated group, but the same were upregulated in ARCE and ARCE+ $H_2O_2$  treated groups and were comparable to that of control group (S2A Fig). mRNA level of proapoptotic gene (*bax*) in H9c2 cells was high in  $H_2O_2$  treated group whereas, the same was less in ARCE and

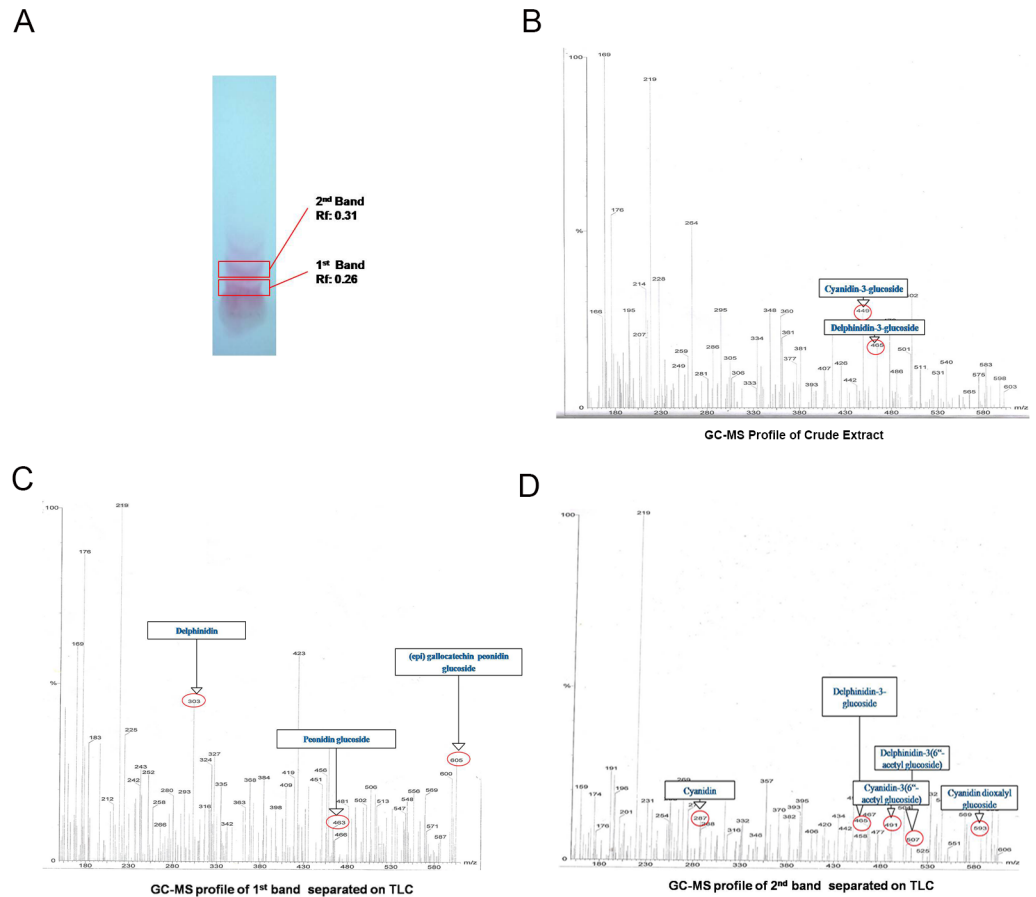


**Fig 1. Characterization of ARCE.** (A) TLC chromatogram of ARCE separated on aluminium silica gel. The spectra represent GC-MS profiles of (B) crude ARCE, (C) 1<sup>st</sup> and (D) 2<sup>nd</sup> bands separated on TLC.

<https://doi.org/10.1371/journal.pone.0182137.g001>

ARCE+H<sub>2</sub>O<sub>2</sub> treated groups. Likewise, anti-apoptotic gene (*bcl-2*) expression was lowered in H<sub>2</sub>O<sub>2</sub> treated group but was relatively higher in ARCE and ARCE+H<sub>2</sub>O<sub>2</sub> treated groups (S2B Fig).

### Gene expression studies in rat cardiac tissue

mRNA levels of intracellular antioxidants (*sod* and *catalase*) were found to be significantly low in ISO treated rats but the same were significantly upregulated in ARCE+ISO group (Fig 4A). Pro-apoptotic gene (*bax*) showed upregulation following ISO treatment whereas, ARCE+ISO treatment could negate the increment with levels comparable to control group. Expression

**Table 2. GC-MS profile of crude extract.**

Peak	Retention Time	Area	Height	Area %
1	9.432	2183807.0	47,715,000	12.32

Peak	Retention Time	Daughter fragment	Parent fragment	Peak identification
1	9.432	-	449	Cyanidin-3-glucoside
			465	Delphinidin-3-glucoside

<https://doi.org/10.1371/journal.pone.0182137.t002>

**Table 3. GC-MS profile of 1<sup>st</sup> band.**

Peak	Retention Time	Area	Height	Area %
1	3.569	706473.9	12,952,837	61.56

**Mass spectrum profile**

Peak	Retention time	Daughter fragment	Parent fragment	Peak identification
1	3.569	463	605	(epi) gallicocatechin peonidin glucoside
2	3.569	481, 303	-	(epi) gallicocatechin delphinidin

<https://doi.org/10.1371/journal.pone.0182137.t003>

**Table 4. GC-MS profile of 2<sup>nd</sup> band.**

Peak	Retention Time	Area	Height	Area %
1	3.55	475339.5	8,855,368	41.59

**Mass spectrum profile**

Peak	Retention Time	Daughter fragment	Parent fragment	Peak identification
1	3.55	287	491	Cyanidin-3(6"-acetyl glucoside)
			593	Cyanidin dioxalyl glucoside
2	3.55	465	507	Delphinidin-3(6"-acetyl glucoside)

<https://doi.org/10.1371/journal.pone.0182137.t004>

level of anti-apoptotic gene (*bcl-2*) was lower in ISO and higher in ARCE+ISO treated groups, (Fig 4B). mRNA levels of *caveolin-3* and *SERCA2a* show a significant decrement in cardiac tissue following ISO treatment whereas, supplementation of ARCE prevented the said decrement as seen in Fig 4C.

### Microscopic observation and plasma CK-MB

ISO treatment accounted for significant increment in Heart: Body weight ratio (HW:BW) and plasma CK-MB levels ( $P < 0.01$ ) (Fig 5A and 5B). However, these parameters were comparable to control in ARCE+ISO treated group. TTC stained sections of ventricular tissue of control rats showed brick red color indicating healthy tissue whereas, that of ISO treated rats was pale in colour with white (necrotic) patches. However, necrotic tissue was minimal in ARCE+ISO

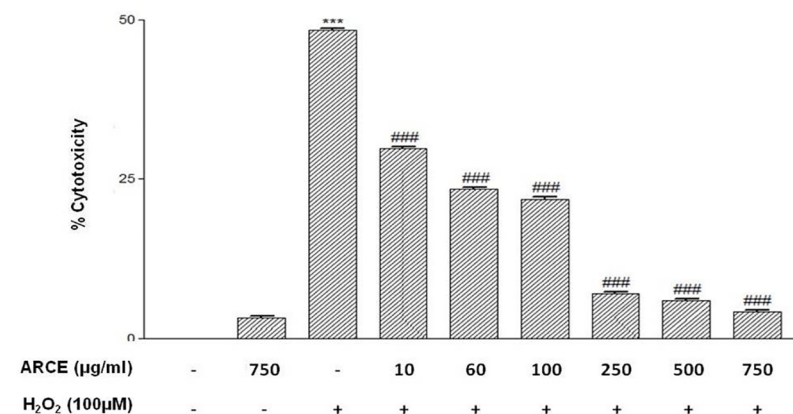


**Fig 2. Effect of ARCE on cytotoxicity in H9c2 cells.** H9c2 cells were treated with H<sub>2</sub>O<sub>2</sub> (100 µM) for 12h with or without pretreatment of ARCE (100–750 µg/ml) for 24 h. Untreated cells were used as control. % Cytotoxicity was determined by MTT Assay. The data were represented as mean ± SEM, for three independent experiments. \*\*\*P<0.001 vs. control group and ### P<0.001 vs. H<sub>2</sub>O<sub>2</sub> group.

<https://doi.org/10.1371/journal.pone.0182137.g002>

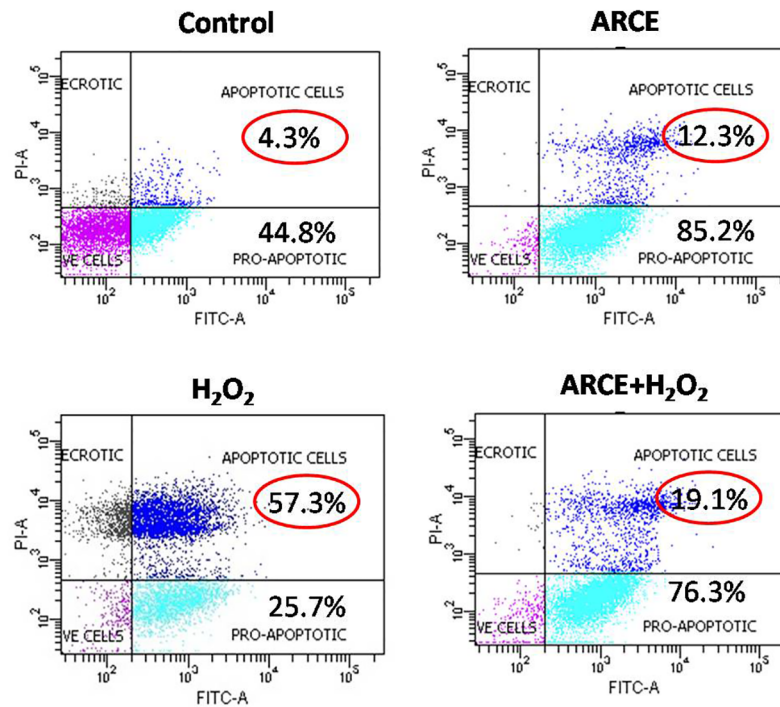


**Fig 3. ARCE prevented H<sub>2</sub>O<sub>2</sub> induced apoptosis in H9c2 cells.** The cells were subjected to various treatments followed by staining with Annexin V-Alexa 488/PI for 15 min at 37°C in dark. Untreated cells were used as control. The stained cells were analyzed by flow cytometer. Double positive events indicate apoptotic cells (values encircled in red) and double negative events indicate viable cell population.

<https://doi.org/10.1371/journal.pone.0182137.g003>

group (Fig 5C). Image analysis of TTC stained ventricular sections in ISO treated rats showed higher percentage of infarct areas compared to ARCE+ISO treated rats. Control group did not show any infarct tissue (Fig 5D). Ventricles of ISO treated rats showed hypertrophy and accounted for more thickness than the control. However, in ARCE+ISO treated rats, it was comparable to that of control (Fig 5E). Haematoxylin-Eosin stained sections of ventricular tissue of ISO treated rats showed gross derangement of myocardial fibres. Whereas, ARCE+ISO treated group showed intact multinucleated fibres identical to that of control (Fig 5F).

### Homology modelling and molecular docking

Thermo-stabilised Turkey  $\beta_1$  Adrenergic Receptor bound to quinoline served as a template showing 69.9% alignment with query Rat  $\beta_1$ AR sequence (S3 Fig). The 3D structure of modelled protein consisted of seven helical structures in bundled formation with flexible loops between Helix-5 (H5) and Helix-6 (H6), residue numbers viz. 258 to 298 (Fig 6A). Ramachandran plot analysis of the model showed that 91.5% residues were in the most favored regions (Fig 6B). Further, D138, S228 and N352 residues in turkey  $\beta_1$  were found to be conserved in Rat  $\beta_1$ AR as per the query template alignment (S3 Fig and Fig 7). Molecular docking of Cyanidin-3-glucoside and Delphinidin-3-glucoside with Rat  $\beta_1$ AR showed that they were well accommodated within the active site and interacted through the hydrophobic and electrostatic bonds at a distance of 2.5 to 3.2 Å. These two anthocyanins accounted for Glide XPG (docking) scores of -8.7 kcal/mol (Fig 8A, 8C and 8E) and -8.5 kcal/mol respectively (Fig 8B, 8D and 8F).

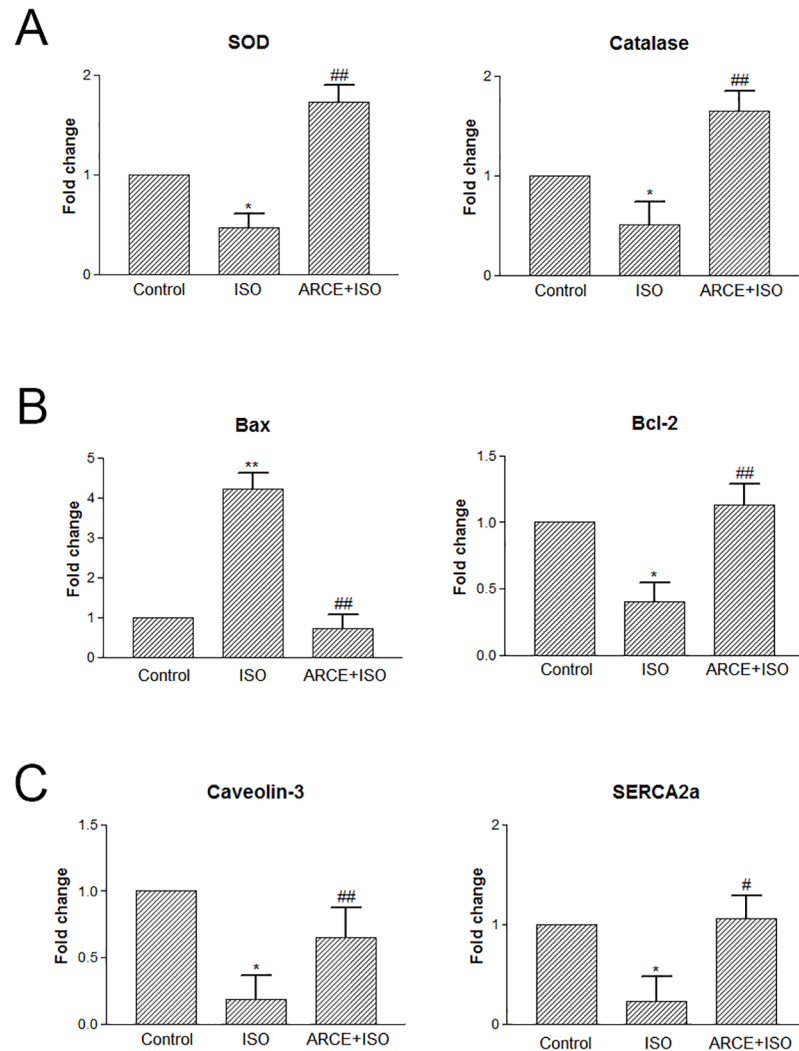


**Fig 4. ARCE prevented ISO induced modulations in gene expressions in rat heart tissues.** The total RNA isolated from heart tissues from rats of various treatment groups were subjected to cDNA synthesis and followed by quantitative PCR for (A) antioxidant genes (*sod* and *catalase*), (B) pro-apoptotic (*bax*) and anti-apoptotic (*bcl-2*) genes and (C) myocardium specific *caveolin-3* and *SERCA2a* were analysed by quantitative PCR. The data were represented as mean  $\pm$  SEM, two independent experiments, n = 6 in each experiments. \*\*P<0.01 and \*P<0.05 vs. control group; ##P<0.01 and #P<0.05 vs. ISO group.

<https://doi.org/10.1371/journal.pone.0182137.g004>

## Discussion

Plant anthocyanins have been extensively studied and reported for their therapeutic properties in human diseases but *in vivo* stability of anthocyanin is always a concern. However, anthocyanins from red cabbage have been reported to have *in vivo* stability as evidenced by the content of its metabolic byproducts detected in urine [29]. Red cabbage is rich in acylated anthocyanins with strong antioxidant activity, stability and therapeutic properties [30]. In our study, red to purple bands obtained in thin layer chromatography of ARCE confirmed presence of anthocyanins [28]. Further, mass spectra obtained by GC-MS revealed presence of cyanidin-3-glucoside and delphinidin-3-glucoside. These results are in agreement with and comparable to the findings of Wiczowski [30].

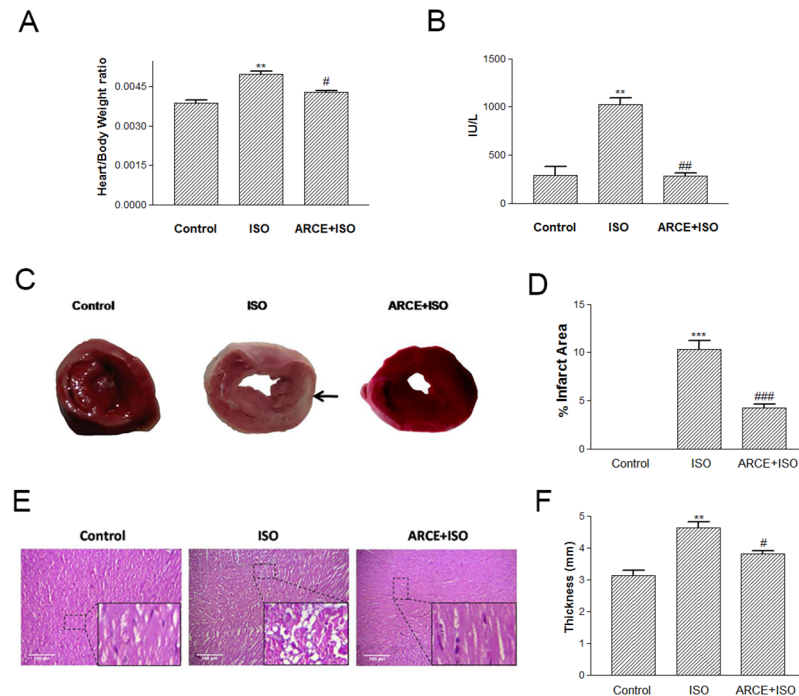


**Fig 5. ARCE prevented ISO induced myocardial damage in rats.** The plots represents (A) the cardiomatic indices (heart weight: body weight) and (B) activity levels of CK-MB of control and treated rats. (C) Representative images of the ventricular tissue sections (control and treated) stained with TTC. Arrows indicate infarcted regions. (D) The plot represents % infarct area as measured from the TTC stained sections using Image J software. Further, the ventricular tissue samples were fixed, dehydrated and subjected to paraffin was embedding. Tissue sections were cut and mounted on the slide. (E) Representative images of the ventricular tissue sections stained with HXE. Magnification = 100X (400X for inset). The data were expressed as mean  $\pm$  SEM from two independent experiments, n = 6 in each experiments. \*\*\*P<0.001 and \*\*P<0.01 vs. control group; ###P<0.001, ##P<0.01 and #P<0.05 vs. ISO group.

<https://doi.org/10.1371/journal.pone.0182137.g005>

Early studies initiated in our lab had reported ARCE mediated decrement in intracellular oxidative stress and restoration of mitochondrial membrane potential in H<sub>2</sub>O<sub>2</sub> treated H9c2 cells [20]. Also, safety evaluations had revealed that ARCE was non-toxic to H9c2 cells (10–100  $\mu$ g/ml) and Swiss albino mice (1000–3000 mg/kg) [20, 31]. Keeping these findings as a background, the present study was initiated to decipher the underlying mechanism of ARCE mediated cardioprotection. Intracellular oxidative stress and resultant mitochondrial membrane damage causes release of cytochrome c and activation of intrinsic apoptotic cascade [32, 33]. In the present study, a dose-dependent reduction in H<sub>2</sub>O<sub>2</sub> induced cytotoxicity and apoptosis of H9c2 cells clearly implicated at ARCE mediated prevention of apoptotic cascade in oxidatively stressed cells. These results are attributable to the free radical scavenging property of ARCE [20] that had accounted for reduced cytotoxicity and prevented trigger of apoptotic cascade.

In rats, isoproterenol had been reported to increase oxygen demand, deplete ATP levels, cause calcium overload and undergo auto-oxidation leading to formation of free radicals [4, 34, 35]. In such a scenario, enzymatic antioxidants (*sod* and *catalase*) have been known to undergo degradation and subsequent exhaustion that furthers the magnimity of oxidative damage within a cell [36]. Therefore, in cardiac tissue ISO induced lipid peroxidation, membrane damage and leakage of CK-MB in plasma are prominent markers of experimentally induced myocardial infarction [37]. In our study, ARCE pretreatment was instrumental in

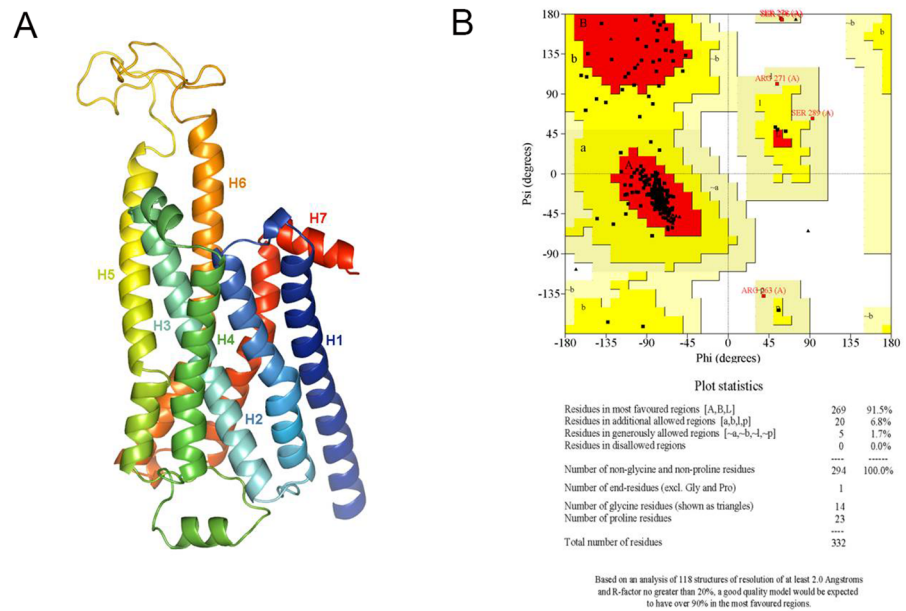


**Fig 6. Homology model of  $\beta_1$ AR.** (A) 3D model of Rat  $\beta_1$ AR showing a bundle structure constitutes of seven helices, the order of helices are marked from N-C terminal as per their respective colours. (B) Ramachandran plot of modelled Rat  $\beta_1$  AR showing stereochemical parameters of each residues present in the structure.

<https://doi.org/10.1371/journal.pone.0182137.g006>

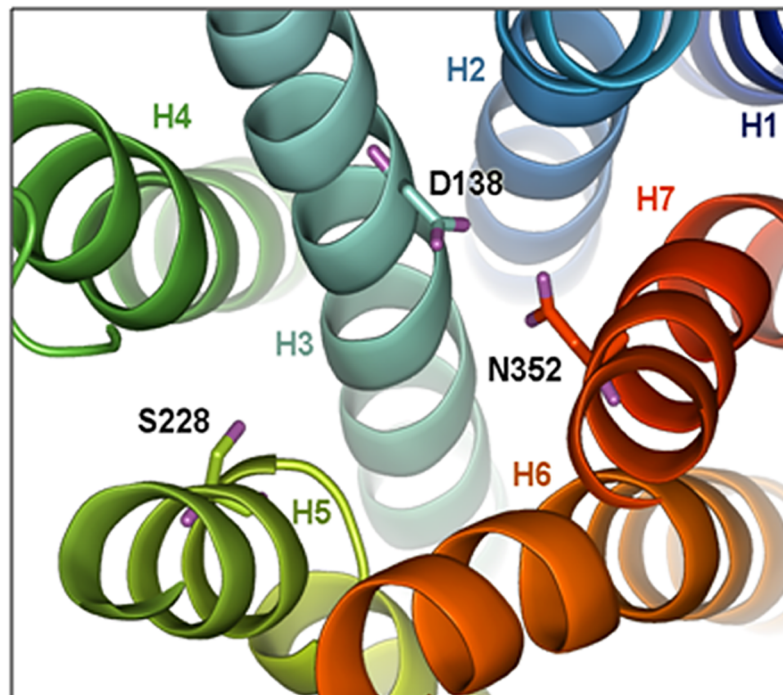


**Fig 7. Active site structure of Rat  $\beta_1$ AR.** Three homologous active site residues (D138, S228a and N352) important for binding quinoline as obtained from the co-crystal structure of Turkey  $\beta_1$ AR (PDB ID: 3ZPR).

<https://doi.org/10.1371/journal.pone.0182137.g007>

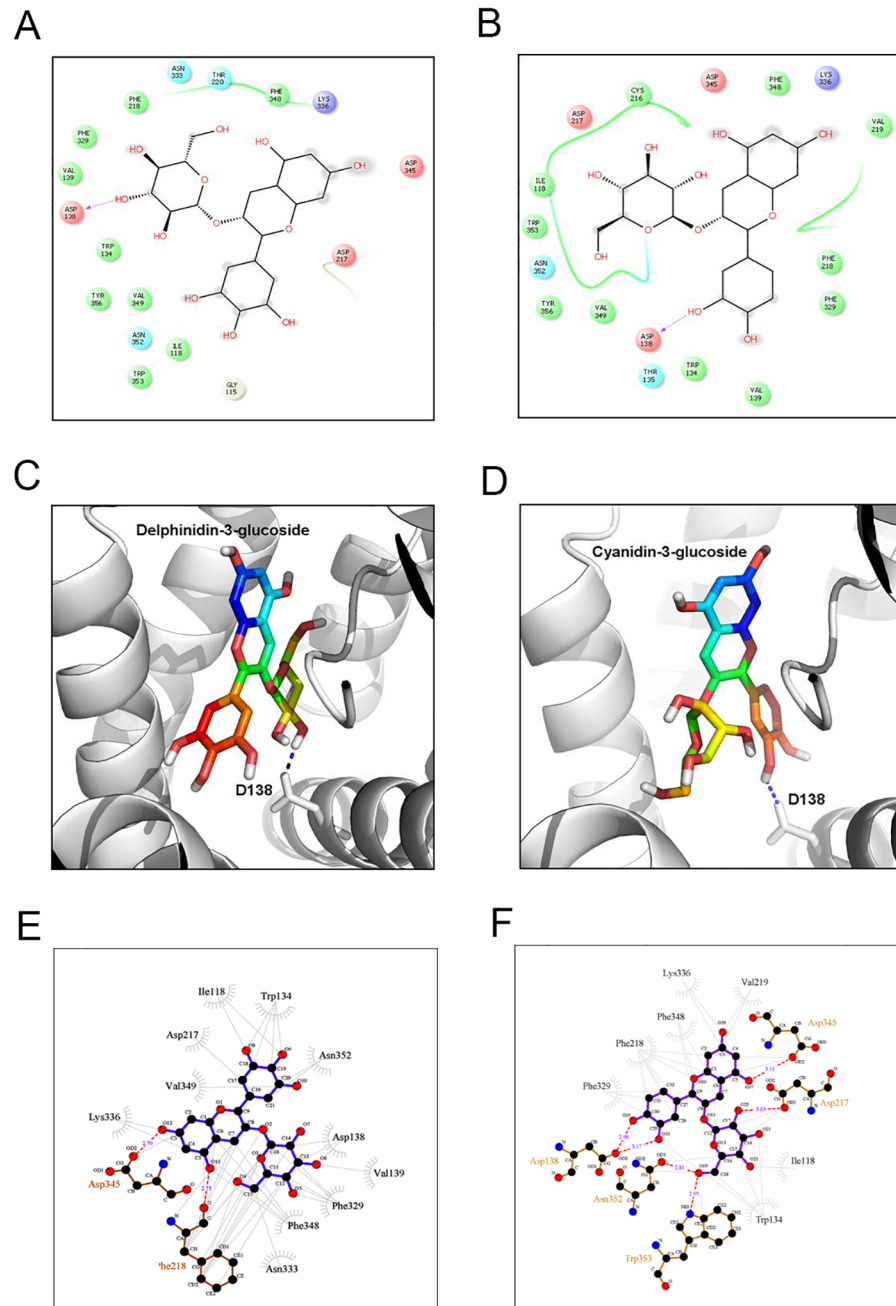


**Fig 8. Molecular interaction of delphinidin-3-glucoside and cyanidin-3-glucoside with Rat  $\beta_1$  adrenergic receptor.** 2D representation of Rat  $\beta_1$ AR with (A) Delphinidin-3-glucoside and (B) Cyanidin-3-glucoside. Residues in green spheres are hydrophobic, blue spheres are positively charged, cyan spheres are polar, and red spheres are negatively charged. The ligand atoms involved in hydrophobic interactions are marked in gray. The purple arrows and their directions represent hydrogen bonds between the ligand and the protein. 3D representations of the interactions are shown for (C) Delphinidin-3-glucoside and (D) Cyanidin-3-glucoside, the Hydrogen bonding with D138 is showing through blue dotted line. (E) LigPlot diagram of Delphinidin-3-glucoside and (F) Cyanidin-3-glucoside.

<https://doi.org/10.1371/journal.pone.0182137.g008>

providing cardioprotection as evidenced by Heart: Body weight ratio, decreased circulating levels of CK-MB, improved levels of enzymatic antioxidants (*sod* and *catalase*) and favourable modulations of apoptotic markers (*bax* and *bcl-2*). Cardiac tissue samples of ISO treated rats showed extensive derangement of cardiac syncytium (HXE staining) and prominent infarcted area (TTC staining). These changes were less pronounced in ARCE+ISO group that also corroborates with the higher levels of mRNA of *sod*, *catalase* and *bcl-2* in this group. Hence, ARCE contributes towards imparting overall cytoprotection to the myocardial tissue. Caveolin, a protein that functions as chaperones and forms little caveolae, plays an important role in signal transduction, vesicular transport, regulation of cholesterol and calcium homeostasis [38, 39]. In cardiomyocytes,  $\beta_1$  adrenergic receptors are concentrated in the caveolae, wherein ISO has been reported to have more affinity for  $\beta_1$  adrenergic receptor with consequential calcium influx, chronotropic-ionotropic imbalance and hypertrophy [40]. In our study, we had recorded upregulation of *caveolin-3* in ARCE+ISO group. This result is attributable to the membrane stabilizing property of ARCE that has also been reported in a study conducted with erythrocytes [17].

CPH models-3.2 server uses profile-profile alignment method guided by secondary structure and exposure predictions to find out best template structure for model building. Thermo-stabilised Turkey  $\beta_1$  adrenergic receptor bound to quinoline was identified as a template with 69.9% sequence identity with our query Rat  $\beta_1$  adrenergic receptor sequence. The active or ligand binding site of Rat  $\beta_1$  adrenergic receptor with loop structures and residues (258–298) was unique but, rest of the residues were conserved as per turkey  $\beta_1$  adrenergic receptor [41]. Further, molecular docking of cyanidin-3-glucoside and delphinidin-3-glucoside with Rat  $\beta_1$  adrenergic receptor showed that they could not only accommodate in the active site, but also could interact through hydrophobic and electrostatic interactions as observed in LigPlot diagram. This further substantiates the effective Glide XPG (docking) scores for cyanidin-3-glucoside and delphinidin-3-glucoside. Hence, these anthocyanins are implied for imparting effective cardioprotection due to the said leads generated from the docking studies.

Previous studies in our lab have reported ISO mediated increase in activity levels of  $\text{Ca}^{+2}$  ATPase in cardiac tissue of rats [42]. Sarcoplasmic Reticulum Calcium ATPase cardiac isoform 2a (*SERCA2a*) has been reported to play a crucial role in control of spatio-temporal patterns of intracellular calcium signalling. ISO mediated stimulation of B-adrenergic receptor activates protein kinase A (PKA) that phosphorylates calcium channels and increases calcium overload within cytoplasm. Ryanodine receptor (RyR) increases net calcium load in cytoplasm due to its efflux from sarcoplasmic reticulum resulting in muscle contraction. *SERCA2a* is instrumental in restoring calcium in sarcoplasmic reticulum therefore, decrement in expression of *SERCA2a* increases cytoplasmic calcium load causing arrhythmia and myocardial damage [43, 44]. This includes altered contraction, hypertrophic growth and apoptosis of cardiomyocytes that have been known to be reverted by upregulation of *SERCA2a*. Hence, merits of *SERCA2a* are also debated as a pharmacotherapeutic target in preventing myocardial infarction [45]. In the present study, ISO treated rat recorded decrement in *SERCA2a* expression whereas; the ones pre-treated with ARCE showed restored *SERCA2a* levels. These observations are significant and add a new dimension to ARCE-*SERCA2a* crosstalk in infarcted myocardium.

## Conclusion

It can be concluded that ARCE manifests multipronged therapeutic effects viz. improving the status of intracellular antioxidants, preventing membrane damage and apoptosis. Also, experimental evidences on alleviation of ISO induced modulations of *caveolin-3* and *SERCA2a* in cardiac tissue by ARCE explains its cardioprotective potential. Molecular docking scores of

cyanidin-3-glucoside and delphinidin-3-glucoside provide insights on their stable interaction with  $\beta_1$  adrenergic receptor and ARCE mediated prevention of myocardial damage. However, lack of information on the crystal structure of rat  $\beta_1$  adrenergic receptor is a possible limitation of the present study. Also, efficacy of ARCE as a cardioprotectant assessed herein is restricted to male rats. A similar experiment with estrogen deficient female rats or variation in age may result in a differential response that needs to be ascertained. Nevertheless, this report throws light on the underlying mechanism of ARCE induced cardioprotection.

## Supporting information

**S1 Fig. GC chromatograms of anthocyanin pigments from (A) crude extract, (B) 1<sup>st</sup> and (C) 2<sup>nd</sup> bands separated on TLC.** The peaks marked in green represent those subjected to further characterization by MS.  
(TIF)

**S2 Fig. ARCE prevented H<sub>2</sub>O<sub>2</sub> mediated antioxidant depletion and apoptotic changes in H9c2 cells.** Total RNA was isolated using TRIzol reagent from treated and control cells and the mRNA levels of (A) antioxidant genes (*sod* and *catalase*) and (B) pro-apoptotic (*bax*) and anti-apoptotic (*bcl-2*) genes were analysed by quantitative PCR. The data were represented as mean  $\pm$  SEM, for three independent experiments. \*\*P<0.01 and \*P<0.05 vs. control group; #P<0.05 vs. H<sub>2</sub>O<sub>2</sub> group.  
(TIF)

**S3 Fig. Alignment of Rat  $\beta_1$ AR (residue 49 to 380) with the template sequence of Turkey  $\beta_1$ AR (PDB ID: 3ZPR) showing critical residues for quinoline binding marked within box.** The actual positions of these residues in Turkey  $\beta_1$ AR are labelled.  
(TIF)

## Acknowledgments

The authors are thankful to University Grant Commission for providing financial assistance in form of Major Research Project (F.No.41-89/2012/SR). We are also thankful to the Co-ordinator, DBTMSUB-ILSPARE, for technical support. Help rendered by Dr. Kishore Rajput for microscopy, Ms. Ramadevi Pulipaka and Ms. Kavita Shirsath is also duly acknowledged.

## Author Contributions

**Conceptualization:** Ranjitsinh Devkar.

**Data curation:** Sarmita Jana, Rahul Mandal.

**Formal analysis:** Sarmita Jana, Shweta Patel, Kapil Upadhyay, Jaymesh Thadani.

**Funding acquisition:** Ranjitsinh Devkar.

**Investigation:** Sarmita Jana, Dipak Patel, Rahul Mandal.

**Methodology:** Sarmita Jana, Ranjitsinh Devkar.

**Project administration:** Ranjitsinh Devkar.

**Supervision:** Ranjitsinh Devkar.

**Validation:** Sarmita Jana, Ranjitsinh Devkar.

**Writing – original draft:** Sarmita Jana, Santasabuj Das, Ranjitsinh Devkar.

**Writing – review & editing:** Sarmita Jana, Shweta Patel, Kapil Upadhyay, Jaymesh Thadani, Rahul Mandal, Ranjitsinh Devkar.

## References

1. Lee Y, Gustafsson ÅB. Role of apoptosis in cardiovascular disease. *Apoptosis*. 2009; 14(4):536–48. <https://doi.org/10.1007/s10495-008-0302-x> PMID: 19142731
2. Santos CX, Anilkumar N, Zhang M, Brewer AC, Shah AM. Redox signaling in cardiac myocytes. *Free Radical Biology and Medicine*. 2011; 50(7):777–93. <https://doi.org/10.1016/j.freeradbiomed.2011.01.003> PMID: 21236334
3. Yeager JC, Iams SG. The hemodynamics of isoproterenol-induced cardiac failure in the rat. *Circ Shock*. 1981; 8(2):151–63. PMID: 7226440.
4. Bloom S, Davis DL. Calcium as mediator of isoproterenol-induced myocardial necrosis. *Am J Pathol*. 1972; 69(3):459–70. PMID: 5086900;
5. Jing L, Wang Y, Zhao XM, Zhao B, Han JJ, Qin SC, et al. Cardioprotective Effect of Hydrogen-rich Saline on Isoproterenol-induced Myocardial Infarction in Rats. *Heart Lung Circ*. 2015; 24(6):602–10. <https://doi.org/10.1016/j.hlc.2014.11.018> PMID: 25533677.
6. Afroz R, Tanvir EM, Karim N, Hossain MS, Alam N, Gan SH, et al. Sundarban Honey Confers Protection against Isoproterenol-Induced Myocardial Infarction in Wistar Rats. *Biomed Res Int*. 2016; 2016:6437641. <https://doi.org/10.1155/2016/6437641> PMID: 27294126;
7. Shih PH, Chan YC, Liao JW, Wang MF, Yen GC. Antioxidant and cognitive promotion effects of anthocyanin-rich mulberry (*Morus atropurpurea* L.) on senescence-accelerated mice and prevention of Alzheimer's disease. *J Nutr Biochem*. 2010; 21(7):598–605. <https://doi.org/10.1016/j.jnutbio.2009.03.008> PMID: 19443193.
8. Qin Y, Xia M, Ma J, Hao Y, Liu J, Mou H, et al. Anthocyanin supplementation improves serum LDL- and HDL-cholesterol concentrations associated with the inhibition of cholesteryl ester transfer protein in dyslipidemic subjects. *Am J Clin Nutr*. 2009; 90(3):485–92. <https://doi.org/10.3945/ajcn.2009.27814> PMID: 19640950.
9. Guo H, Guo J, Jiang X, Li Z, Ling W. Cyanidin-3-O-beta-glucoside, a typical anthocyanin, exhibits antilipolytic effects in 3T3-L1 adipocytes during hyperglycemia: involvement of FoxO1-mediated transcription of adipose triglyceride lipase. *Food Chem Toxicol*. 2012; 50(9):3040–7. <https://doi.org/10.1016/j.fct.2012.06.015> PMID: 22721980.
10. Hidalgo M, Martin-Santamaria S, Recio I, Sanchez-Moreno C, de Pascual-Teresa B, Rimbach G, et al. Potential anti-inflammatory, anti-adhesive, anti/estrogenic, and angiotensin-converting enzyme inhibitory activities of anthocyanins and their gut metabolites. *Genes Nutr*. 2012; 7(2):295–306. <https://doi.org/10.1007/s12263-011-0263-5> PMID: 22218934;
11. Shim SH, Kim JM, Choi CY, Kim CY, Park KH. Ginkgo biloba extract and bilberry anthocyanins improve visual function in patients with normal tension glaucoma. *J Med Food*. 2012; 15(9):818–23. <https://doi.org/10.1089/jmf.2012.2241> PMID: 22870951;
12. Jennings A, Welch AA, Fairweather-Tait SJ, Kay C, Minihane AM, Chowienczyk P, et al. Higher anthocyanin intake is associated with lower arterial stiffness and central blood pressure in women. *Am J Clin Nutr*. 2012; 96(4):781–8. <https://doi.org/10.3945/ajcn.112.042036> PMID: 22914551.
13. Draghici G, Alexandra LM, Aurica—Breica B, Nica D, Alda S, Liana A, et al. Red cabbage, millennium's functional food. *Magnesium*. 2013; 28:26.
14. Wu X, Prior RL. Identification and characterization of anthocyanins by high-performance liquid chromatography-electrospray ionization-tandem mass spectrometry in common foods in the United States: vegetables, nuts, and grains. *J Agric Food Chem*. 2005; 53(8):3101–13. <https://doi.org/10.1021/jf0478861> PMID: 15826066.
15. Scalzo RL, Genna A, Branca F, Chedin M, Chassaing H. Anthocyanin composition of cauliflower (*Brassica oleracea* L. var. botrytis) and cabbage (*B. oleracea* L. var. capitata) and its stability in relation to thermal treatments. *Food Chemistry*. 2008; 107(1):136–44.
16. Igarashi K, Kimura Y, Takenaka A. Preventive effects of dietary cabbage acylated anthocyanins on paraquat-induced oxidative stress in rats. *Biosci Biotechnol Biochem*. 2000; 64(8):1600–7. <https://doi.org/10.1271/bbb.64.1600> PMID: 10993144.
17. Duchnowicz P, Bors M, Podsedek A, Koter-Michalak M, Broncel M. Effect of polyphenols extracts from Brassica vegetables on erythrocyte membranes (in vitro study). *Environ Toxicol Pharmacol*. 2012; 34(3):783–90. <https://doi.org/10.1016/j.etap.2012.09.008> PMID: 23044092.

18. Kataya HA, Hamza AA. Red Cabbage (*Brassica oleracea*) Ameliorates Diabetic Nephropathy in Rats. *Evid Based Complement Alternat Med*. 2008; 5(3):281–7. <https://doi.org/10.1093/ecam/nem029> PMID: 18830445;
19. Sankhari JM, Thounaojam MC, Jadeja RN, Devkar RV, Ramachandran AV. Anthocyanin-rich red cabbage (*Brassica oleracea* L.) extract attenuates cardiac and hepatic oxidative stress in rats fed an atherogenic diet. *J Sci Food Agric*. 2012; 92(8):1688–93. <https://doi.org/10.1002/jsfa.5532> PMID: 22228433.
20. Devkar RV, Pandya AV, Shah NH. Protective role of *Brassica oleracea* and *Eugenia jambolana* extracts against H<sub>2</sub>O<sub>2</sub> induced cytotoxicity in H9C2 cells. *Food Funct*. 2012; 3(8):837–43. <https://doi.org/10.1039/c2fo00001f> PMID: 22592644.
21. Cassidy A, Mukamal KJ, Liu L, Franz M, Eliassen AH, Rimm EB. High anthocyanin intake is associated with a reduced risk of myocardial infarction in young and middle-aged women. *Circulation*. 2013; 127(2):188–96. <https://doi.org/10.1161/CIRCULATIONAHA.112.122408> PMID: 23319811;
22. Glinska S, Gabara B. The effects of the anthocyanin-rich extract from red cabbage leaves on *Allium cepa* L. root tip cell ultrastructure. *Ecotoxicol Environ Saf*. 2011; 74(1):93–8. <https://doi.org/10.1016/j.ecoenv.2010.06.018> PMID: 20650531.
23. Sun X, Sun GB, Wang M, Xiao J, Sun XB. Protective effects of cynaroside against H<sub>2</sub>O<sub>2</sub>-induced apoptosis in H9c2 cardiomyoblasts. *J Cell Biochem*. 2011; 112(8):2019–29. <https://doi.org/10.1002/jcb.23121> PMID: 21445859.
24. Joseph DR. The ratio between the heart-weight and body-weight in various animals. *The Journal of experimental medicine*. 1908; 10(4):521. PMID: 19867145
25. Schmittgen TD, Livak KJ. Analyzing real-time PCR data by the comparative C(T) method. *Nat Protoc*. 2008; 3(6):1101–8. PMID: 18546601.
26. Li C, Gao Y, Xing Y, Zhu H, Shen J, Tian J. Fucoidan, a sulfated polysaccharide from brown algae, against myocardial ischemia-reperfusion injury in rats via regulating the inflammation response. *Food Chem Toxicol*. 2011; 49(9):2090–5. <https://doi.org/10.1016/j.fct.2011.05.022> PMID: 21645579.
27. Thounaojam MC, Jadeja RN, Devkar RV, Ramachandran A. Prevention of high fat diet induced insulin resistance in C57BL/6J mice by *Sida rhomboides* ROXB. extract. *Journal of Health Science*. 2010; 56(1):92–8.
28. Wagner H, Blatt S. *Plant drug analysis: a thin layer chromatography atlas*: Springer Science & Business Media; 1996.
29. Charron CS, Clevidence BA, Britz SJ, Novotny JA. Effect of dose size on bioavailability of acylated and nonacylated anthocyanins from red cabbage (*Brassica oleracea* L. Var. capitata). *J Agric Food Chem*. 2007; 55(13):5354–62. <https://doi.org/10.1021/jf0710736> PMID: 17542615.
30. Wiczowski W, Szawara-Nowak D, Topolska J. Red cabbage anthocyanins: Profile, isolation, identification, and antioxidant activity. *Food research international*. 2013; 51(1):303–9.
31. Thounaojam MC, Jadeja RN, Sankhari JM, Devkar RV, Ramachandran AV. Safety evaluations on ethanolic extract of red cabbage (*Brassica oleracea* L.) in mice. *J Food Sci*. 2011; 76(1):T35–9. <https://doi.org/10.1111/j.1750-3841.2010.01962.x> PMID: 21535729.
32. Grishko V, Pastukh V, Solodushko V, Gillespie M, Azuma J, Schaffer S. Apoptotic cascade initiated by angiotensin II in neonatal cardiomyocytes: role of DNA damage. *Am J Physiol Heart Circ Physiol*. 2003; 285(6):H2364–72. <https://doi.org/10.1152/ajpheart.00408.2003> PMID: 12919932.
33. Ott M, Robertson JD, Gogvadze V, Zhivotovsky B, Orrenius S. Cytochrome c release from mitochondria proceeds by a two-step process. *Proc Natl Acad Sci U S A*. 2002; 99(3):1259–63. <https://doi.org/10.1073/pnas.241655498> PMID: 11818574;
34. Singal P, Kapur N, Dhillion K, Beamish R, Dhalla N. Role of free radicals in catecholamine-induced cardiomyopathy. *Canadian journal of physiology and pharmacology*. 1982; 60(11):1390–7. PMID: 7151008
35. Yeager JC, Whitehurst ME. Verapamil prevents isoproterenol-induced cardiac failure in the rat. *Life Sci*. 1982; 30(3):299–306. PMID: 7070210.
36. Nimse SB, Pal D. Free radicals, natural antioxidants, and their reaction mechanisms. *RSC Advances*. 2015; 5(35):27986–8006.
37. Padmanabhan M, Prince PS. Preventive effect of S-allylcysteine on lipid peroxides and antioxidants in normal and isoproterenol-induced cardiotoxicity in rats: a histopathological study. *Toxicology*. 2006; 224(1–2):128–37. <https://doi.org/10.1016/j.tox.2006.04.039> PMID: 16757080.
38. Li C, Duan W, Yang F, Zhang X. Caveolin-3-anchored microdomains at the rabbit sarcoplasmic reticulum membranes. *Biochem Biophys Res Commun*. 2006; 344(4):1135–40. <https://doi.org/10.1016/j.bbrc.2006.04.024> PMID: 16647041.

39. Roth DM, Patel HH. Role of caveolae in cardiac protection. *Pediatr Cardiol.* 2011; 32(3):329–33. <https://doi.org/10.1007/s00246-010-9881-8> PMID: 21210089;
40. Ostrom RS, Violin JD, Coleman S, Insel PA. Selective enhancement of beta-adrenergic receptor signaling by overexpression of adenylyl cyclase type 6: colocalization of receptor and adenylyl cyclase in caveolae of cardiac myocytes. *Mol Pharmacol.* 2000; 57(5):1075–9. PMID: 10779394.
41. Christopher JA, Brown J, Dore AS, Errey JC, Koglin M, Marshall FH, et al. Biophysical fragment screening of the beta1-adrenergic receptor: identification of high affinity arylpiperazine leads using structure-based drug design. *J Med Chem.* 2013; 56(9):3446–55. <https://doi.org/10.1021/jm400140q> PMID: 23517028;
42. Jadeja RN, Thounaojam MC, Patel DK, Devkar RV, Ramachandran AV. Pomegranate (*Punica granatum* L.) juice supplementation attenuates isoproterenol-induced cardiac necrosis in rats. *Cardiovasc Toxicol.* 2010; 10(3):174–80. <https://doi.org/10.1007/s12012-010-9076-9> PMID: 20509006.
43. Bers DM. Calcium cycling and signaling in cardiac myocytes. *Annu Rev Physiol.* 2008; 70:23–49. <https://doi.org/10.1146/annurev.physiol.70.113006.100455> PMID: 17988210
44. Lipskaia L, Hulot JS, Lompre AM. Role of sarco/endoplasmic reticulum calcium content and calcium ATPase activity in the control of cell growth and proliferation. *Pflugers Arch.* 2009; 457(3):673–85. <https://doi.org/10.1007/s00424-007-0428-7> PMID: 18188588.
45. Lipskaia L, Chemaly ER, Hadri L, Lompre A-M, Hajjar RJ. Sarcoplasmic reticulum Ca<sup>2+</sup> ATPase as a therapeutic target for heart failure. *Expert opinion on biological therapy.* 2010; 10(1):29–41. <https://doi.org/10.1517/14712590903321462> PMID: 20078230